

# Effect of Wheel Slip in the Coordination of Wheeled Mobile Robots<sup>\*</sup>

Shyamprasad Konduri, Edison Orlando Cobos Torres  
Prabhakar R. Pagilla<sup>\*</sup>

<sup>\*</sup> *Mechanical and Aerospace Engineering, Oklahoma State University,  
Stillwater, OK 74078 USA (Tel: 405-740-5900; e-mail:  
pagilla@okstate.edu).*

---

**Abstract:** Motion coordination of differential drive robots with wheel slip is considered in this work. In applications involving motion coordination of multiple wheeled vehicles, much of the existing work has assumed a pure rolling condition between the wheel and ground while deriving the vehicle dynamics and subsequently in the development of model-based controllers that can achieve and maintain the desired formation of vehicles. Wheel slip is common when using differential drive mobile robots as the orientation of the robot is achieved by commanding a velocity differential between the two driven wheels of the mobile robot. In formations of wheeled mobile robots, to maintain the desired spacing between vehicles, rapid accelerations and decelerations may be needed to maintain the desired spacing between vehicles. In this paper, we assume wheel slip and model the dynamics of each mobile robot with a simple Coulomb friction-based traction force model to distinguish between slip and no-slip conditions. Based on this dynamic model of the mobile robot with wheel slip, a formation controller is developed by limiting the torque to the wheel motors of each robot to avoid slip and achieve and maintain the desired formation. Experiments are conducted with a formation that is a platoon of three wheeled mobile robots. Experimental results are shown and discussed to investigate occurrence of wheel slip and its effect on coordination.

---

## 1. INTRODUCTION

Slip between the wheels and the ground can cause considerable deviation from the actual position of a wheeled mobile robot from its desired position. In particular this deviation is exacerbated when measurements from encoders are used to control the wheel angular position which in turn is used to control the Cartesian position and orientation of the mobile robot. Slip is inevitable in differential drive robots because a differential velocity between the left and the right wheels is commanded to achieve an orientation of the wheeled mobile robot in the plane. The slip effect is magnified when coordination of multiple wheeled mobile robots is necessary to achieve and maintain a desired formation with a desired spacing between different robots; an example is a platoon of vehicles where one desires to achieve and maintain a desired spacing between each vehicle in the platoon. A spacing error that is created due to a disturbing force on one particular vehicle may propagate upstream and downstream depending on the location of the vehicle within the formation, the type and form of the communication graph, and the controller on each vehicle that is used to achieve and maintain the formation. To correct for these spacing errors, each mobile robot may typically go through rapid acceleration and decelerations to reject the disturbing forces in an effort to regulate the spacing errors to zero. The rapid acceleration or deceleration of the wheels often leads to wheel slip. This is significant as encoders on driven wheels are often used to

determine the incremental position of the wheeled mobile robot from its start position. If the wheels are slipping, the computation of the Cartesian position of the robot is erroneous as slipping of the wheels will affect the position obtained by using the encoders. This may exacerbate the spacing errors between vehicles in a formation if wheel slip is not taken into consideration in the design of the controller for each vehicle.

It is typical in most of the literature to assume pure rolling conditions while developing the dynamics for the differential drive mobile robot configuration Yun and Yamamoto [1993], Petrov [2010]. Pure rolling of wheels implies that the torque input to the driven wheels is entirely utilized towards the linear movement of the wheel. However, this is not true in many cases where rapid accelerations and decelerations may be involved due to large input torques, which causes the wheels to slip. When a wheel slips only a portion of the applied input torque to the wheels is utilized towards the linear motion of the wheel, this can be determined by studying the wheel-surface interaction and by formulating a traction force model based on this interaction.

There have been many studies related to wheel slip in differential drive robots, such as Sidek and Sarkar [2008], Balakrishna and Ghosal [1995], Y. Tian and Sarkar [2009]. It is typical to derive the kinematics and dynamics of the wheeled mobile robot under slip and traction force expressions are derived for a particular type of wheel-ground interaction. One key aspect in studying wheel slip is the interaction between the wheel and the ground;

---

<sup>\*</sup> This work was supported in part by the US National Science Foundation under Grant No. 0825937.

for example, soft rubber covered wheels, loose soil, etc. Another aspect is the use of caster wheels that are used to support the wheeled mobile robot; one or more caster wheels are used in addition to the two driven wheels to support the robot base platform. Some of the existing work considered either a flexible wheel, rigid ground or rigid wheel, flexible ground to determine the traction force model Sidek and Sarkar [2008], Balakrishna and Ghosal [1995], Y. Tian and Sarkar [2009]; this work has not considered the influence of caster wheels on traction force calculations. Some recent work on wheel slip by considering rigid wheel, rigid ground interaction can be found in Albagul and Wahyudi [2004], Nandy et al. [2011]. In Albagul and Wahyudi [2004] a two stage controller is employed for trajectory tracking and it is indicated that the measurement of the global location of the robot is necessary to effectively control the robot. Traction forces are determined by using the static friction coefficient between the wheel and the ground for both slip and non-slip conditions in Nandy et al. [2011].

Motion coordination of vehicles to create and maintain a formation is a widely researched area in systems and control. Recent work that considers wheel slip in formation control problems can be found in Ze-su et al. [2012], Tian and Sarkar [2012]. In Ze-su et al. [2012] an artificial potential function was used to create an adaptive formation control law for systems with lateral slip and parameter uncertainties; simulation results were presented showing the effectiveness of the controller used. Effect of wheel slip in a leader follower type formation controller was explored in Tian and Sarkar [2012] to show that slip may cause instabilities in otherwise stable formations; simulation results were presented to show this effect. A dynamic model for a differential drive robot with one caster wheel and two driven wheels was derived in Torres et al. [2014] by considering wheel slip. A traction force model is developed by considering the action of the caster wheel (which has been ignored in previous studies) and a simple friction model for both lateral and longitudinal motion.

In this work we consider the problem of motion coordination of wheel mobile robots when there is slip between the wheels and the surface. The dynamics of the robot with both lateral and longitudinal slip of wheels in contact with the surface are considered; the effect of the caster wheel is included in the determination of the traction forces, which can influence the occurrence of slip. Based on the model, a torque limiting strategy is given to avoid slip. A series of experiments are conducted to evaluate the strategy for a platoon of three differential drive robots with the desired velocity profiles chosen such that there is wheel slip. Experimental results are presented and discussed.

The rest of the paper is organized as follows. The dynamics of the differential drive robot with wheel slip is given and discussed in Section 2. Experiments related to investigation of wheel slip in a single robot are discussed in Section 3. Coordination experiments with a platoon of three differential drive robots are discussed in Section 4. Conclusions and future work are given in Section 5.

## 2. WHEEL SLIP IN MOBILE ROBOTS

Consider a sketch of differential drive robot shown in Figure 1. Let the position of the robot be given by the

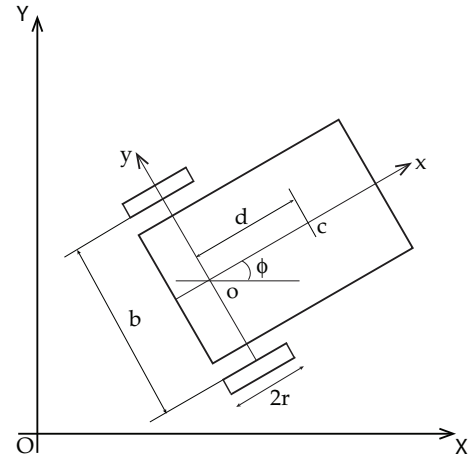


Fig. 1. Two Wheeled Differential Drive Robot

vector  $[x_c, y_c, \phi]^T$ , where  $(x_c, y_c)$  denote the position of point  $c$  (the center of mass) and  $\phi$  is the orientation of the robot in the global coordinate frame. The angular velocity of the wheel is denoted by  $\dot{\theta}$  and subscripts  $r$  and  $l$  denote left and right wheel, respectively. The generalized position vector of the robot is  $q = [x_c, y_c, \phi, \theta_r, \theta_l]^T$ . The control inputs are the wheel torques  $(\tau_r, \tau_l)$ . Let  $s_\phi = \sin \phi$ ,  $c_\phi = \cos \phi$ ,  $b$  is half of the wheel base,  $d$  is the distance between the center of the mass and wheel axis. The kinematics under the pure rolling condition are given by

$$\left. \begin{aligned} \dot{\theta}_r r &= \dot{x}_c c_\phi + \dot{y}_c s_\phi + b \dot{\phi} \\ \dot{\theta}_l r &= \dot{x}_c c_\phi + \dot{y}_c s_\phi - b \dot{\phi} \\ 0 &= \dot{y}_c c_\phi - \dot{x}_c s_\phi - d \dot{\phi} \end{aligned} \right\} \quad (1)$$

Relaxing the pure rolling assumption and letting the wheels slip in both directions, the relationship between linear velocities of the right and left wheels  $(\dot{\rho}_r, \dot{\rho}_l)$  and the lateral velocity of the wheel  $(\dot{\eta})$  to the velocity of the center of mass of the robot can be written as,

$$\left. \begin{aligned} \dot{\rho}_r &= \dot{x}_c c_\phi + \dot{y}_c s_\phi + b \dot{\phi} \\ \dot{\rho}_l &= \dot{x}_c c_\phi + \dot{y}_c s_\phi - b \dot{\phi} \\ \dot{\eta} &= \dot{y}_c c_\phi - \dot{x}_c s_\phi - d \dot{\phi} \end{aligned} \right\} \quad (2)$$

The new generalized position vector describing the robot motion is  $q = [x_c, y_c, \phi, \rho_r, \rho_l, \eta, \theta_r, \theta_l]^T$ . Let  $m_t$  be the total mass of the robot,  $m_w$  be the mass of the wheel,  $F_{long}$  be the longitudinal traction force,  $F_{lat}$  be the lateral traction force,  $r$  be the radius of the wheel,  $I_t$  be the total moment of inertia of the robot in the plane of robot movement,  $I_{wy}$  be the moment of inertia of the wheel in the plane of rotation,  $m_{13} = 2dm_w s_\phi$ ,  $m_{23} = 2dm_w c_\phi$ ,  $O_{n \times n}$  and  $I_{n \times n}$  be the null and identity matrices, respectively.

Define

$$B(q) = [O_{6 \times 2}, I_{2 \times 2}]^T, T = [\tau_r, \tau_l]^T$$

$$f_{11} = (F_{longr} + F_{longl})c_\phi - (F_{latr} + F_{latl})s_\phi$$

$$f_{21} = (F_{longr} + F_{longl})s_\phi + (F_{latr} + F_{latl})c_\phi$$

$$f_{31} = (F_{longr} - F_{longl})b - (F_{latr} + F_{latl})d$$

$$M(q) = \begin{bmatrix} M_1 & O_{3 \times 3} & O_{3 \times 2} \\ M_2 & -I_{3 \times 3} & O_{3 \times 2} \\ O_{2 \times 3} & O_{2 \times 3} & I_{wy} I_{2 \times 2} \end{bmatrix}$$

$$M_1 = \begin{bmatrix} m_t & 0 & m_{13} \\ 0 & m_t & -m_{23} \\ m_{13} & -m_{23} & I_t \end{bmatrix} M_2 = \begin{bmatrix} -s_\phi & c_\phi & -d \\ c_\phi & s_\phi & b \\ c_\phi & s_\phi & -b \end{bmatrix}$$

$$C(q, \dot{q}) = \begin{bmatrix} 2dm_w \dot{\phi}^2 c_\phi \\ 2dm_w \dot{\phi}^2 s_\phi \\ 0 \\ -\dot{\phi}(\dot{x}_c c_\phi + \dot{y}_c s_\phi) \\ -\dot{\phi}(\dot{x}_c s_\phi - \dot{y}_c c_\phi) \\ -\dot{\phi}(\dot{x}_c s_\phi - \dot{y}_c c_\phi) \\ 0 \\ 0 \end{bmatrix} F(q) = \begin{bmatrix} f_{11} \\ f_{21} \\ f_{31} \\ 0 \\ 0 \\ 0 \\ -rF_{longr} \\ -rF_{longl} \end{bmatrix}$$

The dynamics of the robot under slip are given by,

$$M(q)\ddot{q} + C(q, \dot{q}) = B(q)T + F(q) \quad (3)$$

The longitudinal and lateral traction forces and their effect on the wheel are shown in Fig. 2. To calculate the normal

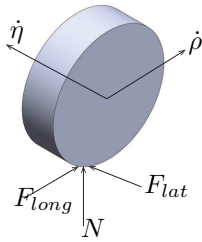


Fig. 2. Longitudinal and lateral slip due to friction forces

forces we assume the robot is constructed such that its mass is uniformly distributed along the longitudinal axis. Therefore, the center of mass lies on the longitudinal axis, and its distance to the center of the caster wheel is defined as  $e$ . We assume that the point at which the caster wheel makes contact with the ground surface when projected onto the robot platform plane falls on the longitudinal axis. One can find relationships of normal forces with the other forces involved using force and moment balance as

$$N_r + N_l + N_{ca} = m_t g \quad (4)$$

$$(F_{latr} + F_{latl})h + N_l b = N_r b \quad (5)$$

$$N_{ca}(d + e) = m_t g d \quad (6)$$

where  $N$  is the normal force,  $g$  is acceleration due to gravity,  $h$  is the height of the center of mass of the robot from the ground, and the subscript  $ca$  in a variable indicates that it is pertaining to the caster wheel.

### 2.1 Slip avoidance control strategy

Consider a wheel that is rotating under pure rolling condition. The total force on the wheel can be expressed in terms of the applied torque ( $\tau$ ) as,

$$F = \frac{\tau m_w r}{m_w r^2 + I_{wy}} \quad (7)$$

For the entire robot we have

$$F = \frac{\tau \frac{m_t}{2} r}{\frac{m_t}{2} r^2 + I_{wy}} = \frac{\tau m_t r}{2I_{wy} + m_t r^2} \quad (8)$$

The value of the maximum force that has to be applied on the wheel before it starts to slip is

$$F_{max} = \mu_s N \quad (9)$$

where  $\mu_s$  is the static friction coefficient. Once the wheel starts to slip the amount of force that is spent on the linear motion of the wheel is given by

$$F_{lin} = \mu_k N \quad (10)$$

where  $\mu_k$  is the kinetic friction coefficient. Thus the difference between the applied force (Equation (7)) and the force given by Equation (10) causes the wheel to continue slipping. Note that lateral slip of the wheel may occur in conjunction with longitudinal slip.

The wheel slip is determined by the traction forces acting on it. Hence using the traction forces if we limit the applied torques on the wheels such that the reaction force is less than the maximum allowable force  $F_{max}$ , slip can be avoided. Thus mathematically the maximum torque that can be applied to the wheel to ensure that there is no slip is obtained by equating Equation (8) to the value  $\mu_s N$  as

$$\tau_{max} = \frac{\mu_s N (2I_{wy} + m_t r^2)}{m_t r} \quad (11)$$

The normal force  $N$  in the above equation is either  $N_r$  or  $N_l$  depending on the wheel in consideration.

## 3. EXPERIMENTS WITH A SINGLE ROBOT

Each wheeled mobile robot has two independent wheels and a free-ball caster wheel for balance, Fig. 3. Each independent wheel is fixed to the shaft of the motor rated at 12 V, with a no-load speed of 350 rotations per minute and a stall torque of 0.78 m-N. A pair of quadrature encoders with 1856 counts per revolution mounted on the shaft of the motor are used to measure the speed of the wheels and calculate the position of the robot. The robot control algorithms are implemented using an Arduino micro-controller along with motor drivers and 'Xbee Series 1' communication module and a desktop computer containing a 'Xbee Series 1' as receiver.

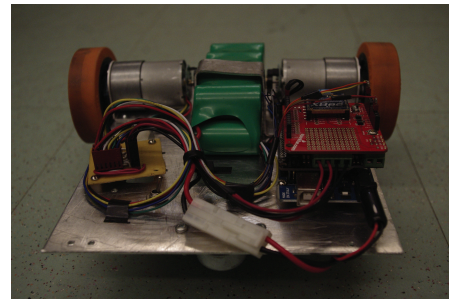


Fig. 3. Mobile robot used in experiments

The control strategy for the robot consists of two loops as shown in Fig 4.

The outer loop is a nonlinear kinematic path controller first proposed in Kanayama et al. [1990]; this outer loop takes the measurement of the robots' current position and

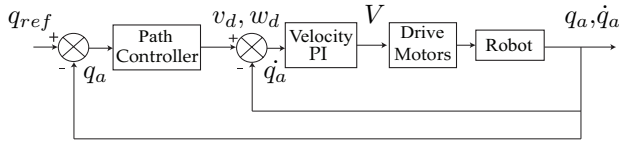


Fig. 4. Two loop trajectory tracking kinematic controller.

the reference trajectory position to calculate the position error. The position error is used to compute the desired linear and angular velocities the robot has to follow to reach the trajectory.

$$v_d = v_r \cos e_\theta + k_x e_x \quad (12a)$$

$$w_d = w_r + v_r(k_y e_y + k_\theta \sin e_\phi) \quad (12b)$$

where  $v, w$  are the linear and angular velocities, respectively, subscripts  $d, r$  denote the desired and reference values and  $k_x, k_y$  and  $k_\theta$  are positive controller gains. The errors  $e_x, e_y, e_\phi$  are computed error in  $x, y$  and  $\theta$  computed in the robots frame. The references values of  $x, y$  and  $\phi$  are obtained from the reference trajectory in the case of a single robot tracking and from the position of the  $(i-1)^{th}$  robot and the desired inter-vehicular spacing in the case of a robots formation. The output of the outer loop provides a velocity reference to the inner velocity loop. The inner loop consists of a Proportional Integral (PI) controller to control individual motor velocities. This inner loop uses the measured motor velocities and reference velocities calculated from  $v_d, w_d$  to generate corrective control voltages.

The parameters for the robots are  $2b = 0.21$  m,  $e = 0.095$  m,  $d = 0.055$  m,  $g = 9.81$  m/s,  $h = 0.0216$  m,  $m_r = 1.5$  kg,  $I_{rz} = 0.009753$  kg m<sup>2</sup>,  $I_{wz} = 0.000584$  kg m<sup>2</sup>,  $I_{wy} = 0.001168$  kg m<sup>2</sup>,  $r = 0.0365$  m,  $m_w = 0.064$  kg. The static and kinetic coefficient of frictions were experimentally. The robot is pulled on the desired surface and the force required to start moving the wheels and to keep the wheels moving is measured. These measured forces and calculated normal reaction force (N) on the wheels is used to compute the coefficients. The friction coefficients thus obtained are  $\mu_s = 0.241$  and  $\mu_k = 0.239$ . Since the two values are very close to each other and the measurement process is prone to uncertainties for all practical purposes both values are taken to be equal to 0.24. Using these numerical values, the maximum allowable torque on each wheel is found to be 0.095 m-N which is equivalent to an acceleration of approximately  $45 \text{ rad/s}^{-2}$ .

The wheels are accelerated for 0.5 seconds using a constant input torque after which the torque is set to zero (i.e., constant velocity). The position of the robot is calculated using the encoder readings. The actual position of the robot is obtained using a video camera looking down from the ceiling above the robot. The position obtained from these two methods is compared to establish the wheel slip in the robot. The robot is run with the maximum motor torque of 0.13 m-N. The position of robot from both encoders and video with and without saturation on the torque input are shown in figures 5 and 6.

Notice that in the case where input torque is not limited the position given by the encoders is more than the true position obtained from the camera. This is because when the wheel slips the linear position traversed by any point on the wheel surface computed using encoder measure-

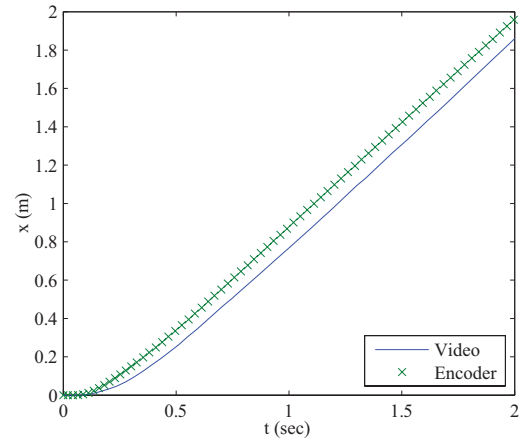


Fig. 5. Evolution of the position of the robot from encoder and video without any limits on input torque

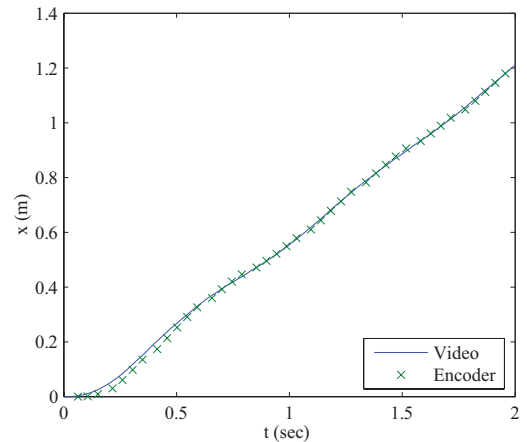


Fig. 6. Evolution of position of robot position from encoder and video with limiting of input torque

ments is more than what is actually observed. Also notice that in the case where the input torque is restricted to less than 0.095 m-N the position obtained from both encoder and video match each other. Such a torque limiting strategy will be applied in coordination experiments next.

#### 4. COORDINATION EXPERIMENTS USING SLIP AVOIDANCE

Coordination experiments are carried out with three robots in a platoon Fig. 7. The first experiment is carried out without any slip avoidance, while the second experiment was done by limiting the input torques. The saturation on input torques can be applied either in the outer loop of controller while calculating the reference velocities for the inner loop or at the end of the inner loop before the voltage is applied to the motors. Although experiments are conducted using both the cases, only a sample of results from the outer loop saturation are provided in this work.

Coordination is introduced into the system from the controller given by equation (12). In the control of a single robot the reference trajectory, i.e., the reference position of the robot  $q_{ref}$  is generated using a reference trajectory function. For coordination the same reference position is obtained by the combination of the neighbor vehicles' position  $q_{i-1}$  and the desired inter-vehicular spacing  $\delta_i$  as

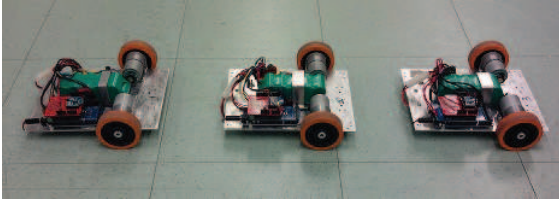


Fig. 7. Picture of mobile robots used in formation experiments

$$q_{ref} = q_{i-1} - \delta_i$$

The communication between robots follows a ring structure as discussed in Konduri et al. [2013], i.e., each robot transmits its position only after it receives the position from its neighbor.

The inter-vehicular communication is crucial for the effective functioning of the formation. Any delay in communication may lead to large accelerations resulting in slip. Consider a straight line trajectory parallel to the x-axis and let there be a spacing error only in the x-direction. Then if one were to use the controller discussed previously, the equation (12) will reduce to

$$v_d = v_r + k_x(x - x_r) \quad , w_d = 0$$

If there is a communication delay  $\tau_d \geq 0$ , then the desired linear velocity can be written as

$$v_{dd} = v_r e^{-\tau_d} + k_x(x - x_r e^{-\tau_d}) \quad (13)$$

From the above equation,

$$\begin{aligned} |v_{dd}| &\leq |v_r e^{-\tau_d}| + k_x |x - x_r e^{-\tau_d}| \\ &\leq |v_r| + k_x |x - x_r| + k_x |x_r| (1 - e^{-\tau_d}) \end{aligned} \quad (14)$$

Since  $k_x > 0$  and  $(1 - e^{-\tau_d}) > 0$ ,  $k_x |x_r| (1 - e^{-\tau_d}) \geq 0$ . Hence  $|v_{dd}| > |v_d|$  for all  $x_r \neq 0$  and the magnitude of  $v_{dd}$  keeps increasing with  $x_r$  and  $\tau_d$ . If the inner loop follows the desired velocities instantaneously, delay in communication can cause sharp accelerations which in turn will result in slip. Notice that as the formation size increases the delay time may increase further increasing the desired velocity corrections.

The position through out the experiments is obtained from the encoders and the final positions after the vehicles stop at the end is measured manually. In both the experiments the outer loop control runs at 20 Hz and the inner loop runs at 50 Hz. The encoder ticks are accumulated separately using interrupts and the number of counts are obtained every time when either the inner or outer loop runs.

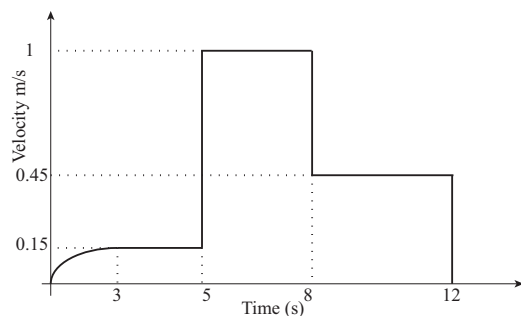


Fig. 8. Velocity profile used in experiments

The experiments started with zero inter-vehicular spacing error and the coordination controller starts after 3 seconds into the experiment. The starting position for robots are (0.6096, 0), (0,0) and (-0.6096, 0) meters with orientation 0 degrees. The desired inter-vehicular spacing is set to 0.6096 m. The velocity profile used for the experiments is shown in Fig 8.

The evolution of the x-position of the robots without limiting the torque are shown in Fig 9. Notice that the rate of change of position increases around 5 seconds into the experiment and decreases after 8 seconds and finally goes to zero after 12 seconds into the experiment. The experiment is run for one acceleration and one deceleration however the deceleration is smoother than the acceleration phase. The x-position of the robots with torque limiting strategy is shown in Fig. 10.

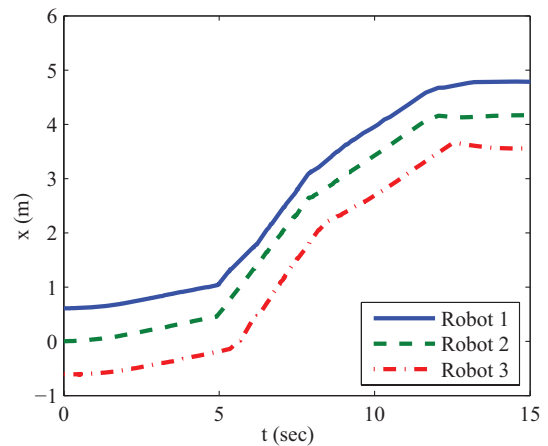


Fig. 9. Evolution of robot x positions (meter) without slip avoidance

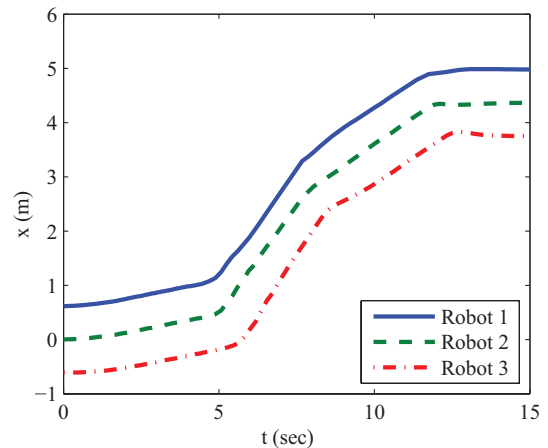


Fig. 10. Evolution of robot x positions (meter) with slip avoidance

Comparing the position one can clearly see that in the case of limiting the input torques, the positions change more smoothly than the case without such torque limits, in particular during accelerations and decelerations. Also observe that when limiting input wheel torque, the inter-vehicular spacings are maintained better. The evolution of y-positions for both cases is shown in Figs. 11 and 12. Observe that the error in the y-position as measured by the

encoders is substantially less when torque limiting strategy is employed.

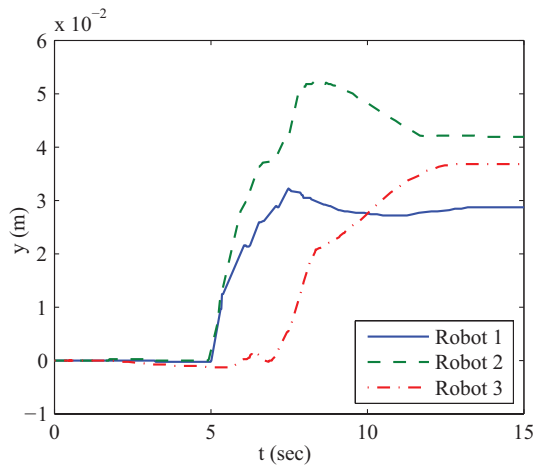


Fig. 11. Evolution of robot y positions (meter) without slip avoidance

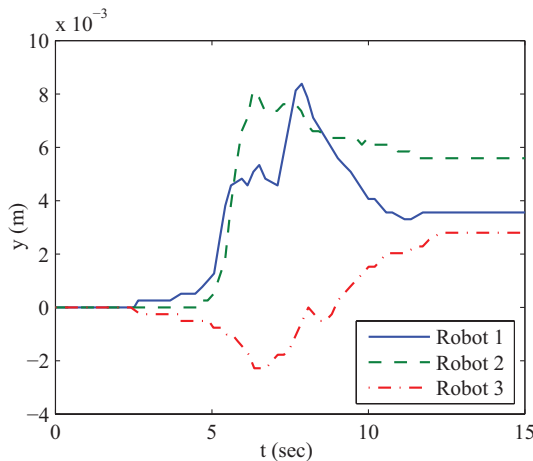


Fig. 12. Evolution of robot y positions (meter) with slip avoidance

The final positions of the three robots from encoder and manual measurement without limiting torque are (4.78, 0.02), (4.17, 0.04), (3.55, 0.03) and (4.87, 0.24), (4.26, 0.18), (3.65, 0.42). Notice that the x-positions are within 0.1 meters where as the y-position has larger error. The final positions with slip avoidance are (4.97, 0.003), (4.36, 0.005), (3.75, 0.002) and (5.02, 0.07), (4.38, 0.06), (3.77, 0.06). Comparing the measurements shows that when limiting torque to avoid slip, the errors in both x and y are much smaller. When input torques are constrained as given by the traction force model, wheel slip is avoided thereby improving the accuracy of position measurement and reducing the spacing errors.

## 5. CONCLUSION

In this work we have investigated wheel slip and its effect on coordination of multiple mobile robots. A torque limiting strategy is employed to restrict the torques that would cause slip, which is based on the dynamic model where slip is explicitly included. Extensive experiments were

conducted to evaluate and verify the proposed method. Possible future work on this topic include online estimation of friction coefficients, implementation of coordination trajectories that involve changing orientation of the robots, and development of an advanced nonlinear controller that includes the robot dynamics and the traction forces.

## REFERENCES

- A. Albagul and Wahyudi. Dynamic modeling and adaptive traction control for mobile robots. In *Proceedings of 30th Annual Conference of IEEE Industrial Electronics Society*, volume 1, pages 614–620 Vol. 1, 2004.
- R. Balakrishna and A. Ghosal. Modeling of slip for wheeled mobile robots. *IEEE Transactions on Robotics and Automation*, 11(1):126–132, 1995.
- Y. Kanayama, Y. Kimura, F. Miyazaki, and T. Noguchi. A stable tracking control method for an autonomous mobile robot. In *Proceedings of IEEE International Conference on Robotics and Automation*, pages 384–389 vol.1, 1990.
- S. Konduri, P.R. Pagilla, and S. Darbha. Vehicle formations using directed information flow graphs. In *American Control Conference (ACC), 2013*, pages 3045–3050, 2013.
- S. Nandy, S.N. Shome, R. Somani, T. Tanmay, G.Chakraborty, and C.S.Kumar. Detailed slip dynamics for nonholonomic mobile robotic system. In *International Conference on Mechatronics and Automation*, pages 519–524, 2011.
- P. Petrov. Modeling and adaptive path control of a differential drive mobile robot. In *Proceedings of the 12th WSEAS international conference on Automatic control, modelling & simulation*, pages 403–408, 2010.
- N. Sidek and N. Sarkar. *Dynamic Modeling and Control of Nonholonomic Wheeled Mobile Robot Subjected to Wheel Slip*. PhD thesis, Vanderbilt University, 2008.
- Y. Tian and N. Sarkar. Formation control of mobile robots subject to wheel slip. In *IEEE International Conference on Robotics and Automation (ICRA)*, pages 4553–4558, 2012.
- E.O. Cobos Torres, S. Konduri, and P.R. Pagilla. Study of wheel slip and traction forces in differential drive robots and slip avoidance control strategy. In *American Control Conference (ACC)*, June 2014.
- N. Sidek Y. Tian and N. Sarkar. Modeling and control of a nonholonomic wheeled mobile robot with wheel slip dynamics. In *IEEE Symposium on Computational Intelligence in Control and Automation*, pages 7–14, 2009.
- X. Yun and Y. Yamamoto. Internal dynamics of a wheeled mobile robot. In *Proceedings of IEEE/RSJ International Conference on Intelligent Robots and Systems*, volume 2, pages 1288–1294 vol.2, 1993.
- Cai Ze-su, Zhao Jie, and Cao Jian. Formation control and obstacle avoidance for multiple robots subject to wheel-slip. *Int J Adv Robot Syst*, 9, 2012.